Досліджено вплив зміни геометрії дна шпуру (свердловини) на виникнення і розвиток початкових тріщин в гранітному масиві при детонації заряду вибухової речовини. Чисельне моделювання швидкоплинних процесів дозволяє отримати додаткову інформацію про складні фізичні явища, яка недоступна при експериментальних методах досліджень. В даний час найбільш перспективним методом моделювання і розрахунку таких задач є метод скінченних елементів

Ключові слова: свердловина, перебур, концентратор напружень, буропідривні роботи, метод скінченних елементів, AUTODYN

Исследовано влияние изменения геометрии дна шпура (скважины) на возникновение и развитие начальных трещин в гранитном массиве при детонации заряда взрывчатого вещества. Численное моделирование быстропротекающих процессов позволяет получить дополнительную информацию о сложных физических явлениях, которая недоступна при экспериментальных методах исследований. В настоящее время наиболее перспективным методом моделирования и расчета таких задач является метод конечных элементов

Ключевые слова: скважина, перебур, концентратор напряжений, буровзрывные работы, метод конечных элементов, AUTODYN

UDC 622.235.534
DOI: 10.15587/1729-4061.2017.101444

SIMULATION OF DYNAMIC FRACTURE OF THE BOREHOLE BOTTOM TAKING INTO CONSIDERATION STRESS CONCENTRATOR

V. Vorobyov
Doctor of Technical Sciences, Professor
Department of Mechanics and Materials Science*
E-mail: vvv.imit@gmail.com
M. Pomazan
PhD
Department of Geodesy,
Organization of Land Use and cadastre*
S. Shlyk
PhD, Associate Professor
Department of Manufacturing Engineering*
E-mail: svshlyk@gmail.com
L. Vorobyova
PhD, Associate Professor
Department of Economics*
E-mail: larivorobiova@gmail.com
*Kremenchuk Mykhailo Ostrohradskyi National University
Pershotravneva str., 20, Kremenchuk, Ukraine, 39600

1. Introduction

Currently, over 80 % of rock volumes are destroyed in open rock mining with drilling and blasting operations (DBO), which predetermine efficiency of all subsequent processes of mineral mining and processing. Costs of drilling and blasting operations in the total cost of a unit of extracted rock mass measure up to 15–25 % [1].

In blasting practice, elongated explosive charges are widely used for both open and underground mining of minerals. Explosion of such charges results in a motion of gaseous detonation products possessing certain features: 90 % of the detonation wave energy is directed at an angle of 70...80° to the longitudinal axis of the borehole and 10 % along it [2]. Such a motion of the detonation wave does not contribute to the maximum transformation of the wave energy into the work of nucleation of initial microcracks in the borehole walls and a significant part of it is uselessly transferred to the lower layers of the rock body. Thus, the so-called «sleeves» are formed which can only be avoided by means of subdrilling. Depending on the physical and mechanical properties of the rock body, its length varies from 2 to 4 m [3].

Essential shortcomings of subdrilling are as follows:

1) longer time and higher drilling costs (20...30 % higher cost of drilling works and explosives);

2) a significant part of explosives is placed in the subdrilling. As a result, the charge is removed from the rock body to be crushed which worsens crushing of the upper part of the hole shoulder and increases yield of oversize pieces;

3) increase in crack formation in the upper part of the underlying shoulder. This adversely affects drilling holes in it, reduces productivity of drilling rigs to two times and increases quantity of oversized pieces [3].

Proceeding from this fact, elimination of subdrilling will reduce consumption of explosives and improve the charge work, especially for the first-row boreholes. In addition, absence of subdrilling will significantly reduce drilling work volumes.

A closer attention to studying the processes occurring at the borehole bottom contributes to a more effective execution of drilling and blasting works. Taking into account a significant share of expenses for drilling and blasting operations in the unit cost of production, these activities are relevant.

2. Literature review and problem statement

In destruction of rocks, stress concentrators are of great importance. Artificial creation of various notches or incisions in the body in a mechanical or explosive way [4] can significantly reduce the load required for rock fracture. The conducted studies show that the peak stresses are largely determined by the defect curvature (hole curvature in this case), they can exceed many times the value of the stresses in a solid plate at the curvature apex [5].

$$\tau = \tau_0 \left(1 + 2\sqrt{\frac{l}{\rho}} \right), \quad (1)$$

where τ_0 is the fracture stress in absence of defects, Pa; l is the notch depth, m; ρ is the curvature radius at the notch apex, m.

Numerous studies, mainly related to metal parts, have shown that expression (1) is valid not only for elliptical holes, but also for holes and defects of any shape on the contour of which there are points with a small curvature radius.

Application of this effect to improve efficiency of rock destruction was mainly limited to a directed splitting. Studies [6] have shown that it is possible to eliminate the shortcomings connected with the use of subdrilling by intensifying development of transverse cracks forming at the drillhole bottom while simultaneously reducing intensity of pinning along the charge axis. The desired effect can be achieved by applying the methods used in directed splitting, one of which is artificial violation of the material continuity in a specified direction. To improve the process of working the notch bottom, an incision should be formed at the junction of the borehole walls and bottom in a form of a ring in the base plane [6]. The ring notch can be formed by a mechanical or explosive method. Annular notching at the junction between the borehole walls and bottom facilitates formation of an initial horizontal crack in the bottom zone. Further, gaseous detonation products (DP) lengthen this crack by penetration into it. Presence of a crack already formed in the given crack zone will contribute to a strengthening of the quasi-static action of gaseous DP at the bottom section of the borehole and an achievement of the design plane of rock separation.

However, formation of a ring notch in the bottom of the borehole is a difficult task, special drilling equipment is required which entails longer duration and higher costs of drilling operations.

It is possible to refuse from subdrilling thru the use of borehole explosive charges intended for crushing rocks and having an air cushion in the lower part of the charge, which provides a normal working of the shoulder foot. An intensive destruction of the rock body in the lower part of the borehole and its better crushing are realized due to the interaction of shock waves formed by the air gap.

Theoretical studies [7] show that when detonation products flow through the air cushion, an incident shock wave propagates in front of which a pressure of about 200–300 kg/cm^2 arises depending on the type of explosive. The incident shock wave is reflected after reaching the well bottom. At the same time, a reflected shock wave propagates through the explosion products in front of which a sharp pressure growth takes place. Thus, the effect of a double shock wave in the lower part of the well, which results in a repeated pressure can create favorable conditions for better processing of the shoulder foot which enables 50 % less subdrilling or even its complete abandonment.

When loading watered wells, dispersal with tamping or other materials should be avoided as this material gets into the charge and leads to worsening the detonation ability or a failure of the charge detonation. The most practically feasible and cheap way at present is making air gaps of foamed polystyrene.

One of the simplest methods requiring no additional expenses for lessening subdrilling consists in the use of the effect of meeting detonation waves to strengthen action of explosion in the bottom part of the borehole. Placement of two charges in such a way that the detonation waves can meet at the shoulder foot can ensure a significant growth of pressure [8].

To eliminate the problem of subdrilling, new designs of borehole explosive charges based on the change of motion direction of the shock wave and gaseous DP have been developed recently. This is achieved by placement of a shock wave concentrator (SWC) in the bottom of the well [9]. The disadvantage of SWC is burnout of loose explosives. In addition, shock wave and DP change their motion direction to an angle other than 90°. As a result, a part of explosion energy is expended on the useless shaking of the rock body, which leads to a decrease in the utilization rate of the borehole. The use of SWC is complicated in horizontal and inclined boreholes because it is unsteady and will fall on the borehole wall.

To develop new methods for improvement of the shoulder foot, a deep physics study of the processes occurring at the hole bottom is necessary. The most economically feasible way to achieve results in this direction is the use of mathematical modeling. To study fast processes, software complexes, which apply explicit methods of solving equations of continuous medium mechanics, have become widely used at present.

ANSYS AUTODYN is an analytical tool for solving explicitly formulated problems for modeling complex nonlinear dynamics of solids, liquids, gases and interactions between them. It is a powerful tool for interdisciplinary calculations in explicitly formulated problems providing a wide range of modeling capabilities including high-speed impacts or explosion. AUTODYN has proven itself in the tasks of ballistic loading of materials. Simulation of behavior of such materials is impossible without taking into account complex anisotropic elastoplastic character of behavior, nonlinear nature of shock-wave compression, and anisotropic fracture with the effects of progressive loss of strength. AUTODYN's ability to connect hydrodynamic and strength solvers also enables simulation of combined explosion and fragmentation effects on the structures.

3. The aim and tasks of research

The study objective was to assess the effect of geometry of the borehole bottom in a granite body during explosive detonation on distribution of stresses and growth of an initial annular crack.

To achieve this objective, the following tasks were set:

– evaluate influence of the rounding radius on the parameters of the formed initial crack;

– determine the nature of change in the length of the initial crack depending on the rounding radius;

– investigate effect of the rounding radius on the change in the width of the initial crack.

4. The procedure of studying the effect of the borehole bottom geometry in detonation of an explosive charge

In the present study, computer simulation of the effect of the rounding radius at the borehole bottom in a granite body was carried out during detonation of the explosive charge on distribution of stresses and growth of the initial annular crack. Four cases were considered: with a cylindrical borehole shape and a toroidal shape with radii of rounding 10, 20 and 40 mm. The system includes atmospheric air, a sand tamping, a charge of explosives and a granite body. The geometric dimensions of the model in the longitudinal section are shown in Fig. 1.

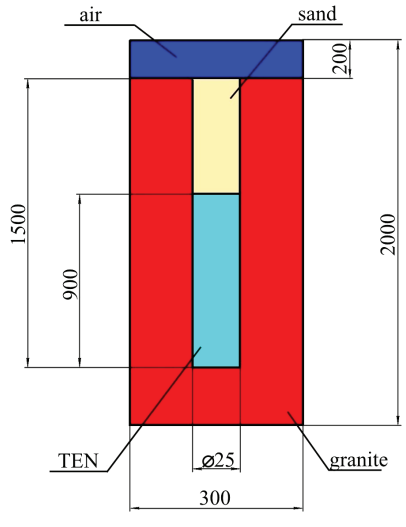

Fig. 1. Structure of the model (dimensions are given in cm)

The process of detonation is numerically described by a general system of differential equations. The equations consist of the laws of conservation of mass, momentum, energy, additional equations and real models of explosive, air, sand and granite. Real models play an important role connecting strain and internal energy. Fluids and gases are modeled to a sufficient degree by the equation of state (EOS) which expresses the relationship between pressure p, specific volume V and specific energy e. Additional equations are needed for modeling solids since solids have shear resistance.

To model complex dynamic processes in AUTODYN, there is a possibility of a common use of various numerical methods that best suit the specifics of each part of the problem. For example, one type of solver can be used in one task to calculate fluid and gas flows, and another one to calculate the structure strength. At the same time, interaction of all parts in space and time was organized within the framework of a single program.

AUTODYN solvers can be divided into the following categories: Lagrangian, Euler, ALE (arbitrary Lagrangian-Euler method), SPH (smoothed particles method). For the correct choice of a solver, two criteria must be considered: accuracy and productivity. Tables 1, 2 show basic and additional equations of solvers, respectively [10]. Table 3 shows definitions and units of variables.

Table 1

Conservation laws in the basic equations of AUTODYN solvers

Conservation laws	Lagrangian description	Euler description
Mass	$\frac{d\rho}{dt}+\rho\frac{\partial v_i}{\partial x_i}=0$	$\frac{\partial\rho}{\partial t}+\frac{\partial(\rho v_i)}{\partial x_i}=0$
Moment	$\frac{dv_i}{dt}=f_i+\frac{1}{\rho}\frac{\partial\sigma_{ij}}{\partial x_i}=0$	$\frac{\partial v_i}{\partial t}+v_j\frac{\partial v_i}{x_i}=f_i+\frac{1}{\rho}\cdot\frac{\partial\sigma_{ij}}{\partial x_j}$
Energy	$\frac{dE}{dt}=-\frac{p}{\rho}\cdot\frac{\partial v_i}{\partial x_i}+\frac{1}{\rho}s_{ij}\varepsilon'_{ij}$	$\frac{\partial E}{\partial t}+v_i\frac{\partial E}{\partial x_i}=-\frac{p}{\rho^2}\left(\frac{\partial\rho}{\partial t}+v_i\frac{\partial\rho}{\partial x_j}\right)+\frac{1}{\rho}s_{ij}\varepsilon'_{ij}$

Table 2

Additional equations for modeling in AUTODYN solvers

Stress tensor	$\sigma_{ij}=-(p+q)+s_{ij}$
Equation of state (EOS)	$p=f(\rho,e)$
Determining model	$\sigma_{ij}=g(\varepsilon_{ij},\varepsilon'_{ij},E,D)$
Detonation	$h(p,\rho,v,T,x,t)=0$

Table 3

Definitions and variable units

Symbol	Unit	Definition
t	s	time
v	m/s	velocity
x	m	displacement
D	–	destruction
E	J	internal energy
p	Pa	hydrostatic pressure
s	Pa	compression stress
T	K	temperature
q	Pa	pseudoviscous pressure
ρ	kg/m^3	density
σ	Pa	stress
ε	–	strain
i, j, k, 0	–	Initial state
With a stroke	–	time derivative

With Lagrange's approach to the description of motion of a continuous medium, the computational grid is «frozen» into the material, it moves and deforms simultaneously with it (Fig. 2). Lagrangian solvers are the most accurate and effective method for calculating nonlinear problems of dynamic loading of structures. The main drawback of the Lagrangian methods is excessive distortion and «entanglement» of the computational grid at large deformations leading to loss of accuracy in these areas and sometimes to a complete termination of calculation. In AUTODYN, this problem can be partially solved by using an artificial erosion algorithm, which removes excessively deformed elements from the calculation.

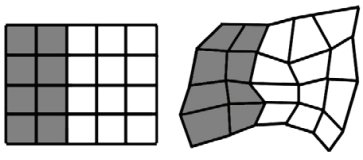

Fig. 2. Computational grid in the Lagrangian representation: *a* — at the initial moment of time; *b* — under loading

The Euler solvers use computational grids that are rigidly fixed in space. The medium motion is formed by the flow of materials from one cell to another (Fig. 3). This approach avoids the problems associated with the grid distortion. Therefore, Euler solvers are ideally suited for calculating flows of a medium with large deformations, especially fluid flows and gases. AUTODYN includes two types of Euler solvers: a multicomponent Euler solver designed to simulate the flow of several materials, and a one-component specialized Euler solver for calculating air shock waves (Euler-FCT (Flux Corrected Transport)) which enables calculation of flows of only one material with the perfect gas equation.

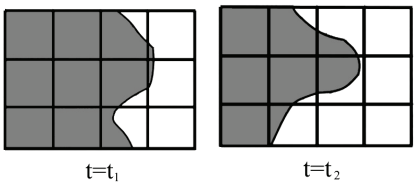

Fig. 3. Computational grid in the Eulerian representation: *a* — under the action of loading; *b* — with the development of loading

ALE, like the Lagrangian method, uses grids moving together with the material. At the same time, it combines the best aspects of the Lagrangian and Euler approaches. The use of Euler algorithms is reduced to alignment and correction of the computational grid. Alignment of the grid makes it possible to avoid the procedure of artificial erosion and can be effectively used for explosive loading of structures.

AUTODYN also includes the gridless Lagrange method of smoothed particles SPH (Smooth Particle Hydrodynamics). The main area of its application is calculation of high-speed interactions as well as modeling destruction and fragmentation of brittle materials, such as ceramics, concrete, etc. [11].

A unique feature of the AUTODYN software package is the possibility of combining contact algorithms and Lagrangian-Euler coupling in one calculation, which makes it possible to carry out a complex analysis of the combined loading of structures for the action of shock wave and fragmentation effects.

AUTODYN has its own library of materials but the sand model presented in the library is not sufficient to simulate the release of sand tamping into environment and there are no tetranitropentaerythritol (TEN) and granite in the library. Therefore, the possibilities of creating and modifying materials available in the library can be used.

To determine the model of sand, use the data obtained in work [12]. The model was obtained for sand with 6.57 % moisture content. The model was obtained by means of a triaxial compression, which made it possible to measure velocities of waves in a sand sample. A brief description of the sand model is presented in Table 4 and in Fig. 4–6.

Table 4

Sand model parameters

Parameter	Unit	Value	Note
Density	g/cm^3	2.641	
Equation of state (EOS)	–	compaction	Fig. 4, 5
Strength model	–	granulated	Fig. 6
Fracture model	–	hydrotension	p_{min} = –1 kPa (sand has a zero compaction)

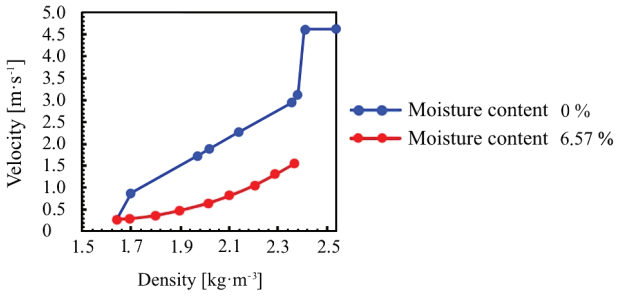

Fig. 4. Velocity vs. density graph for sand (the blue line is the dependence according to work [12])

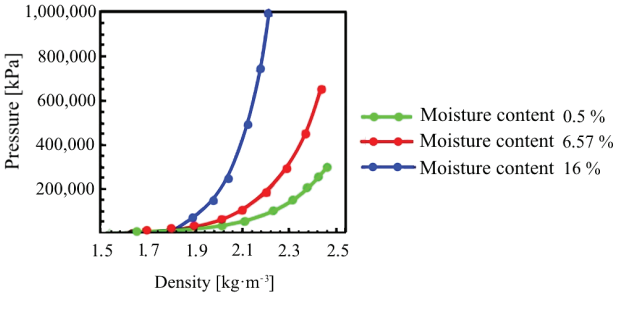

Fig. 5. Pressure vs. density graph for sand

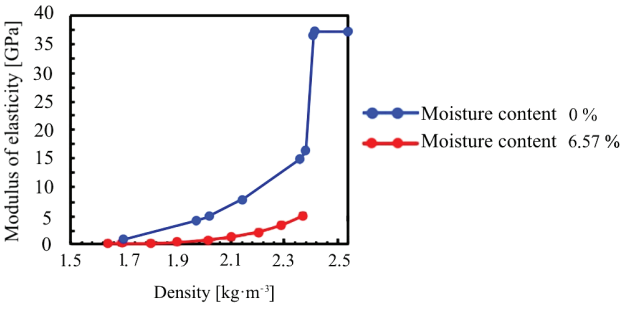

Fig. 6. Modulus of elasticity vs. density graph for sand (the blue line is the dependence according to work [12])

In determining the properties of the granite model, guidance with the data given at the resource [13] and in works [14–16] can be used. The main quantities describing behavior of granite under loading are given in Table 5 and in Fig. 7, 8.

Table 5

Parameters of the real model describing behavior of granite

Parameter	Unit	Value
Density	g/cm^3	2.66
Equation of state (EOS)	–	Polynomial
Compression modulus	GPa	43.87
Temperature	K	300
Specific thermal capacity	J/kg	654
Equation of strength	–	Riedel, Hiermaier and Thoma (RHT) model
Shear modulus	GPa	17
Compression strength	MPa	150
Tensile strength	–	0,05
Shear strength	–	0,07
Tension/compression ratio	–	0.72
Brittle-viscose transition	–	0.01
Crack formation constant, B	–	2.50
Crack formation constant, M	–	0.85
Compression strain rate constant	–	0.025
Compression strain rate limit	–	0.045
Model of fracture	–	Riedel, Hiermaier and Thoma (RHT) model
Fracture constant, D1	–	0.025
Fracture constant, D2	–	1.000
Minimal fracture strain	–	0.060
Residual shear modulus	–	0.250
Model of the fracture stretch	–	Hydro
Model of erosion	–	Plastic strain

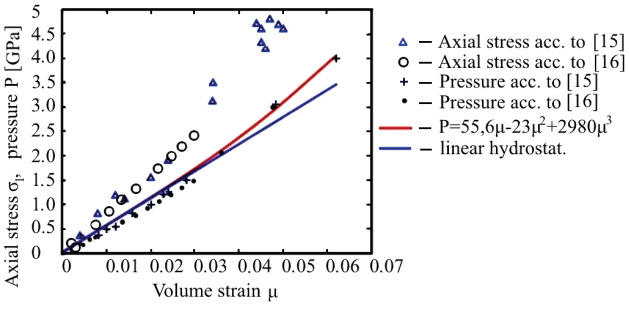

Fig. 7. Data of impact loading tests and granite reaction in systems «axial stress σ_1 – volume strain μ» and «pressure P – volume strain μ»

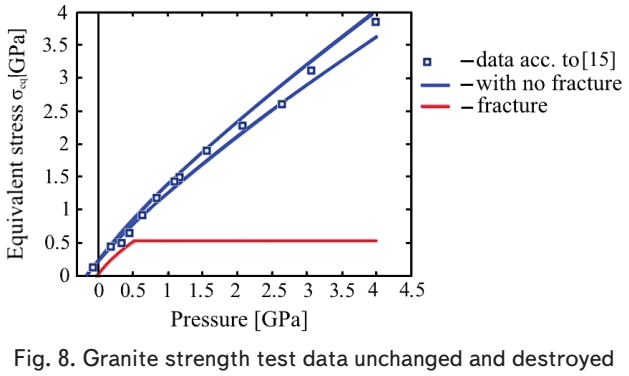

Fig. 8. Granite strength test data unchanged and destroyed

Set properties of the explosive (TEN) model according to works [17, 18] (Table 6).

Table 6

Parameters of the real model describing behavior of TEN explosive

Parameter	Unit	Value
Density	kg/m^3	1620–1773
Velocity of detonation	m/s	8200–8700
Flash temperature	°C	220
Decomposition temperature	kJ/kg	5756
Brisance (Gess)	mm	24
Brisance (Cast)	mm	3.5
Minimal density factor	–	$1{\cdot}10^{-6}$
Minimal density factor (Smoothed Particle Hydrodynamics, SPH)	–	0.20
Maximal density factor (SPH)	–	3.00
Minimal velocity of wave propagation	m/s	10^{-6}
Maximal velocity of wave propagation (SPH)	m/s	$1.01{\cdot}10^{20}$
Maximal temperature	K	$1.01{\cdot}10^{20}$
Equation of state (EOS)	–	Jones-Wilkins-Lee (JWL) model
Autoconversion into ideal gas	–	yes

In the presented model, flow out boundary was used as a boundary condition. This condition allows the material to leave the calculated region under loading, that is, reflection is not allowed at this boundary. Granite and its environment (atmospheric air) expanding under the influence of explosive loading can freely cross the boundaries of the model without reflection. This boundary condition can be only applied to the material for which Euler's solver is used.

A two-dimensional axisymmetric model with rotation around the x axis was developed using a multi-solver. To increase accuracy of the results, millimeters, milligrams, milliseconds were used as basic units of measurement. Four equidistant initiation points of explosion initiation were added to the system, their step of response time was $3.1296{\cdot}10^2$ ms taking into account the detonation velocity. An initial condition equal to $2.068{\cdot}10^5$ was added to the air body; it gives the air pressure equal to 1 atmosphere. An additional condition was also applied to the whole system in a form of gravity the vector of which is directed along the x axis. The scheme of the model with coordinates of the node points in the coordinate system x; y is shown in Fig. 9.

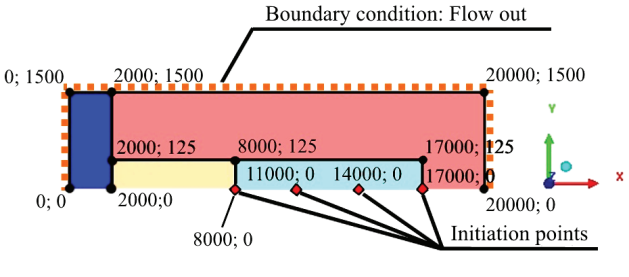

Fig. 9. Configuration of the model of explosion in the granite borehole

An important step in the model compilation is construction of a finite-element grid. The dimensions of atmospheric air grids and the charge of explosives can be neglected. The granular structure of sand and the requirements to the accuracy of calculating formation and growth of fracture sites in a granite body require an introduction of a larger number of cells. The increase in the number of cells in the model enables obtaining of a more adequate simulation result (Fig. 10) but it significantly increases the task calculation time, especially in low-performance systems.

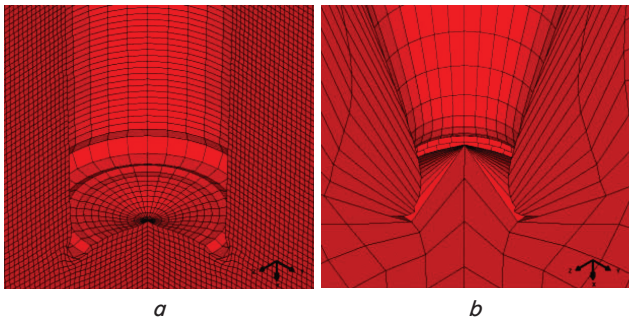

a *b*

Fig. 10. Comparison of the result of calculating the initial crack growth in a granite body when the model rotates by 270° around the axis of symmetry: *a* — for smaller size of the finite element grid cell; *b* — for larger size of the finite element grid cell

As a result of trial calculations, the following optimal conditions for constructing finite element grids of the model components were selected (Table 7).

Table 7

Basic parameters of the finite element calculation grid

Element	Solver type	Finite element dimensions, mm			The number of:	
		Length	Width	Height	Nodes	Cells
Air	Euler	50	50	50	1.271	1.200
Sand tamping	Euler	5	5	5	31.226	30.000
Explosive charge	Euler	5	5	5	46.826	45.000
Granite body	Lagrange	10	10	10	271.951	270.000
Total:					351.274	346.200

To solve the fracture problem, a personal computer with a Intel Core i5 CPU having the clock speed of 2.60 GHz and RAM memory space of 4 GB was used. For the indicated parameters of the computational model, solution of the problem under the condition of limiting time of 8 ms (about 25.000 calculation cycles) took about eight hours of continuous operation. The total amount of occupied disk space for solving the problem at a condition of writing the saved files every 0.01 ms of the calculated process was about 900 MB.

5. The results obtained in modeling fracture of the borehole bottom during detonation of the explosive charge

As the calculation results have shown, kinetic energy of the explosive charge was exhausted in about 3 ms and its further change occurred only due to reflection of the shock wave from the hole walls and the sand tamping (Fig. 11). This indicates completion of the process of the explosive detonation by this time.

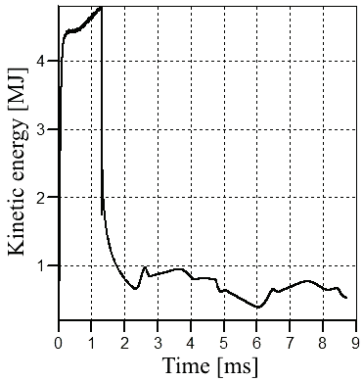

Fig. 11. Change in time of the kinetic energy of the explosive charge

However, as the graph of the change in the speed of displacement of the nodes in the grid located near the borehole bottom shows (Fig. 12), further displacement of the grid nodes was occurring.

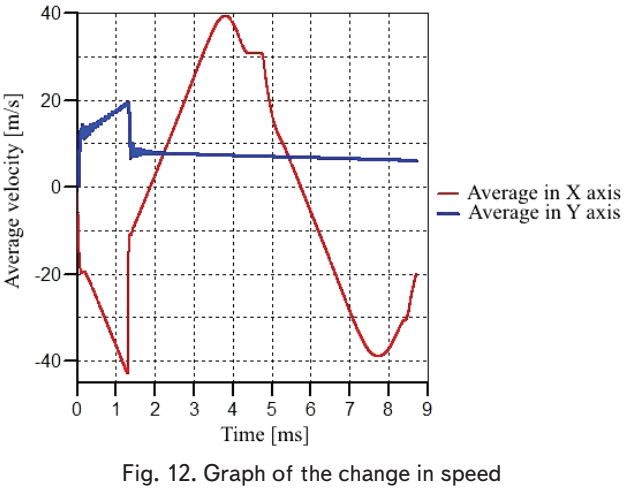

Fig. 12. Graph of the change in speed of displacement of nodes of a finite-element grid of the granite body

This indicates a continuation of deformation of the body parts and further growth of cracks under the action of inertia forces and accumulated stresses. As can be seen from the obtained stress diagrams (Fig. 13–16), the change in stresses and crack growth in all four cases have ceased approximately at the time point equal to 7–8 ms.

The obtained diagrams make it possible to conclude that even when the strain growth ceases, considerable accumulated stresses are observed in all cases.

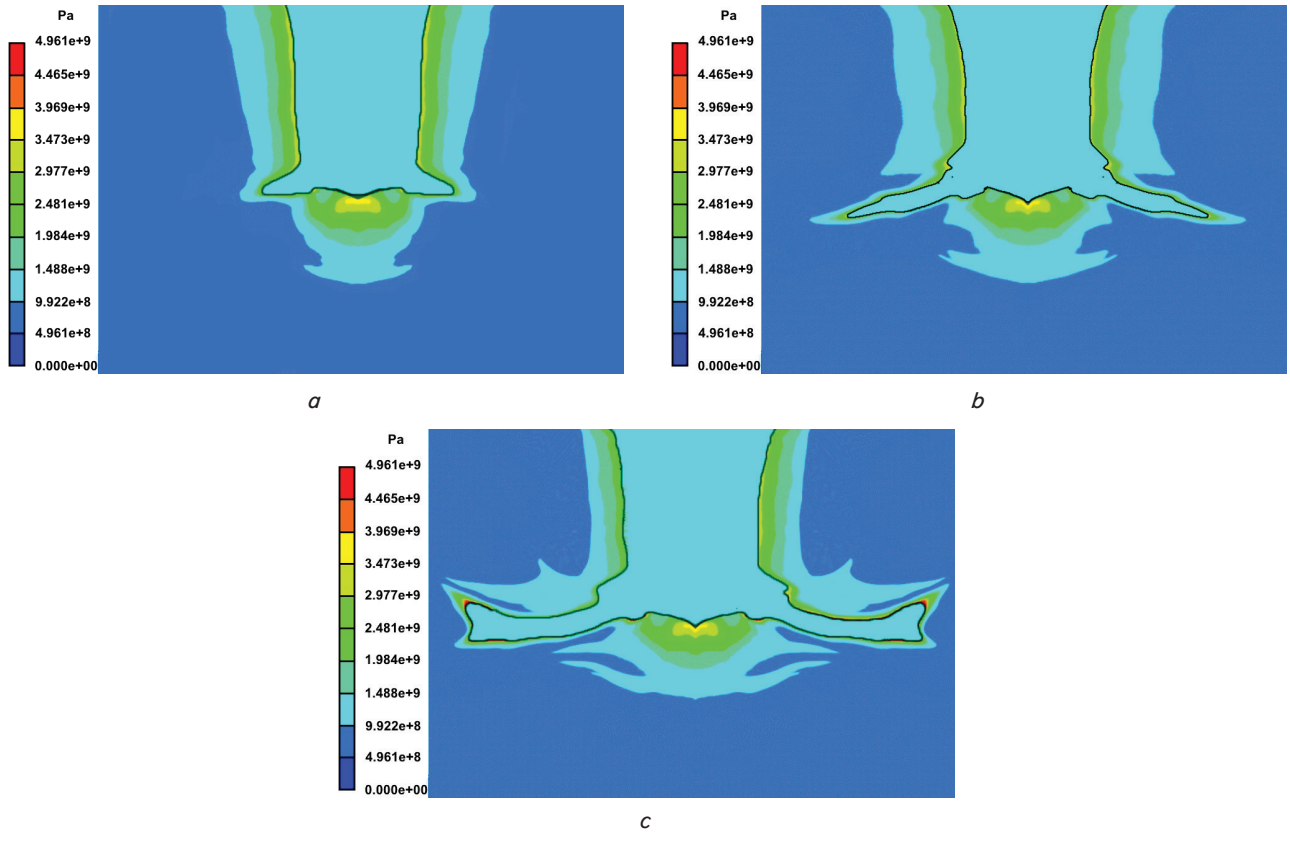

Fig. 13. Growth of the crack and a diagram of normal stresses at $r_{cr} \rightarrow 0$ at the point of time:
a – 2.321 ms; *b* – 4.643 ms; *c* – 6.964 ms

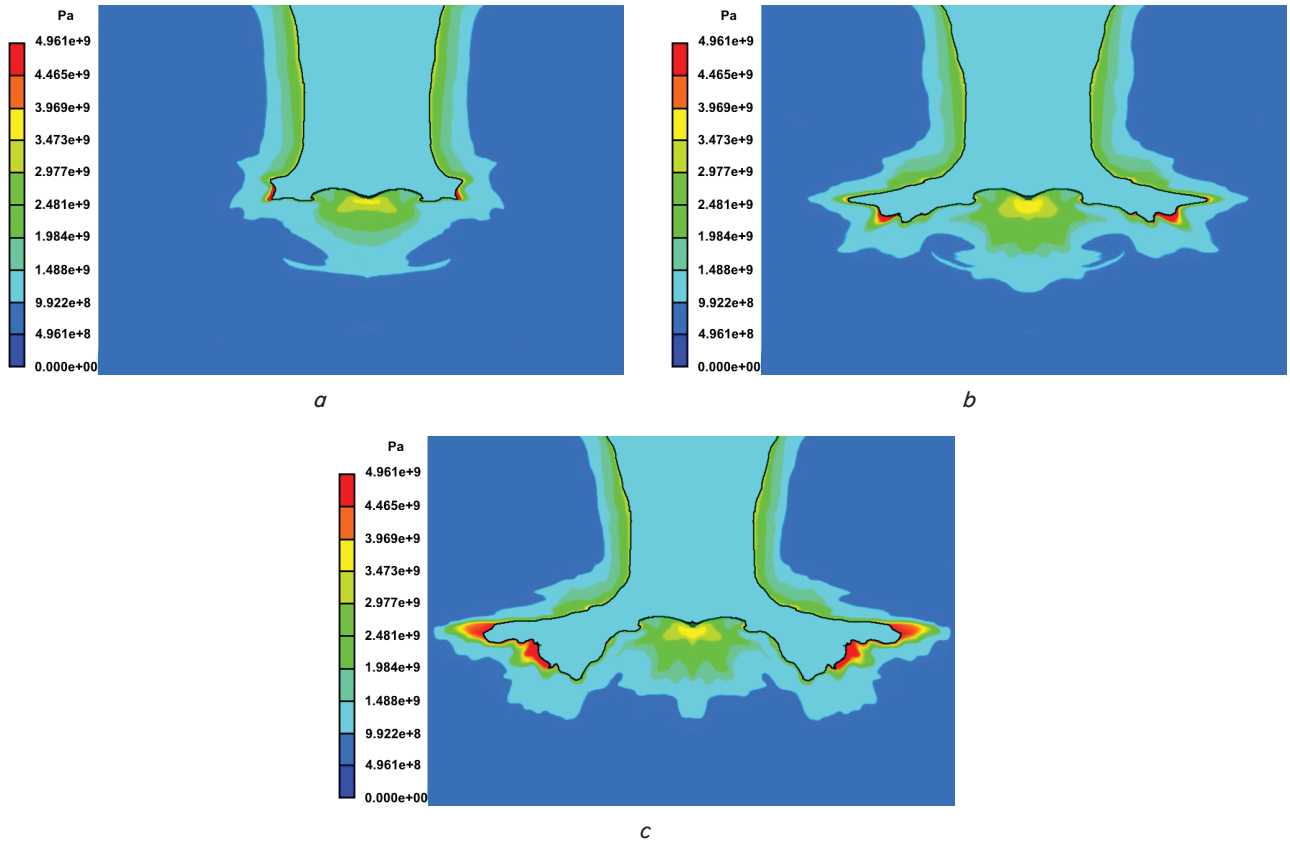

Fig. 14. Growth of the crack and a diagram of normal stresses with the bottom rounding radius of 10 mm at the point of time:
a – 2.375 ms; *b* – 4.751 ms; *c* – 7.125 ms

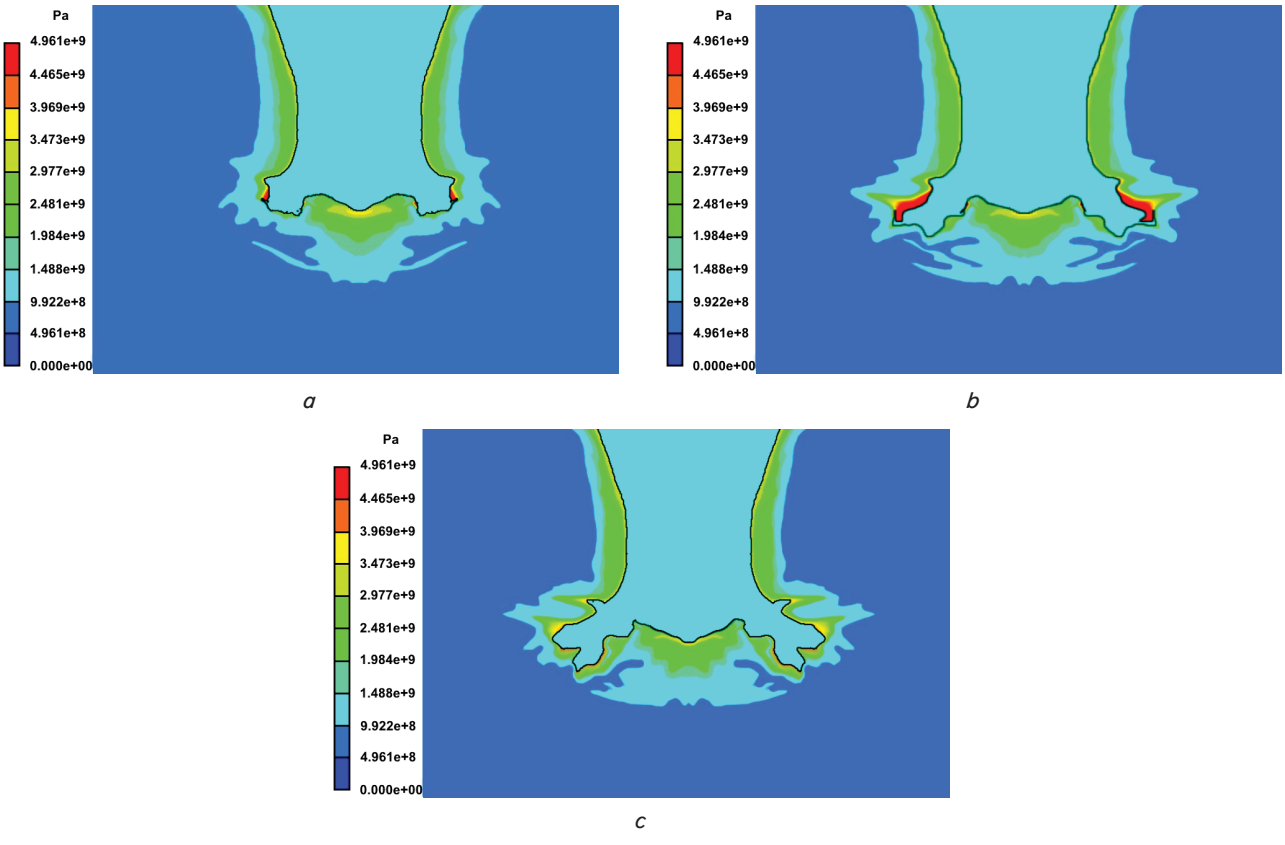

Fig. 15. Growth of the crack and a diagram of normal stresses with the bottom rounding radius of 20 mm at the point of time: *a* – 2.371 ms; *b* – 4.741 ms; *c* – 7.112 ms

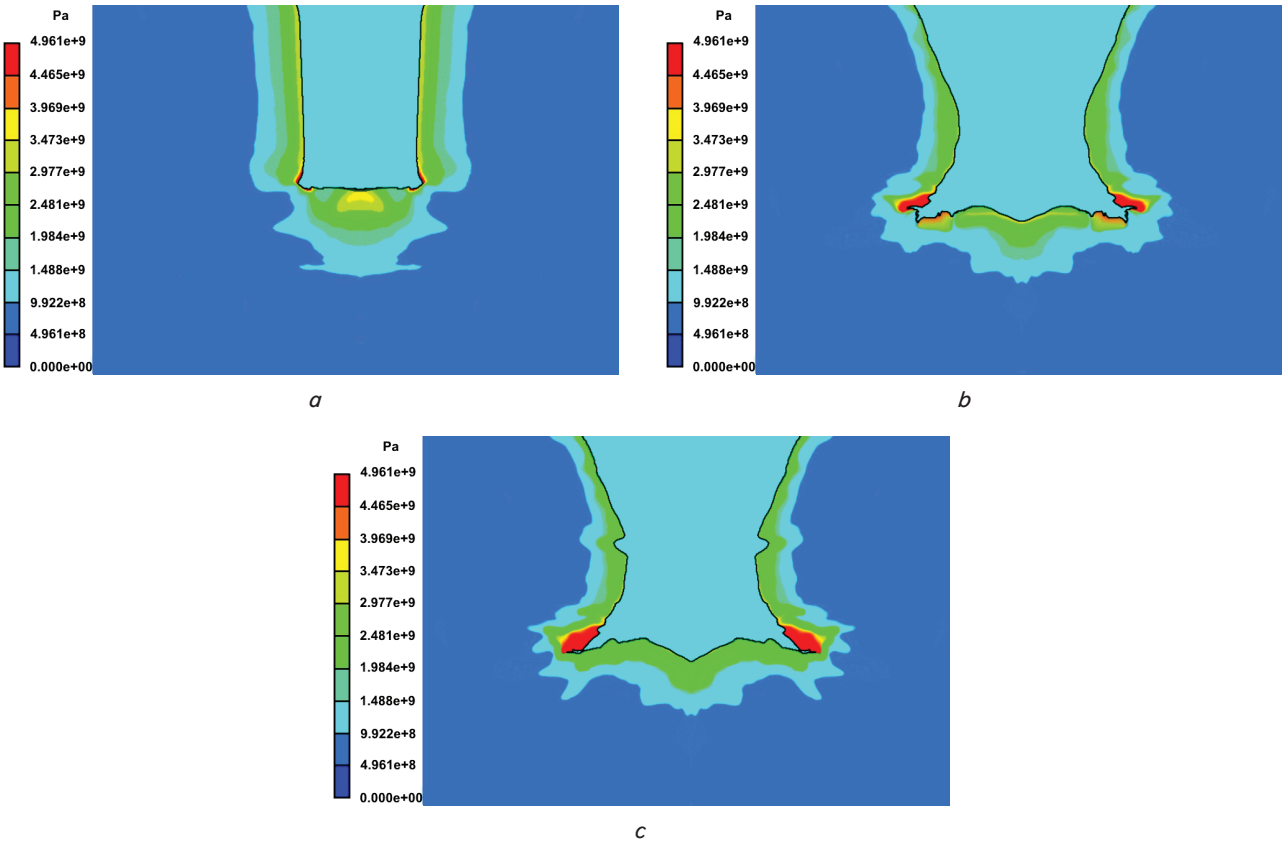

Fig. 16. Growth of the crack and a diagram of normal stresses at the bottom rounding radius of 40 mm at the point of time: *a* – 2.655 ms; *b* – 5.309 ms; *c* – 7.964 ms

6. Discussion of the results obtained in modeling effect of the borehole bottom geometry on the character of the well fracture

As it was mentioned earlier, one of the features of the Lagrangian solver is the rigid coupling of the finite element grid to the material and their joint movement and deformation. This type of solver calculates movement of the grid nodes under the action of explicit loading (detonation of the explosive charge and expansion of the detonation products) but does not take into account spontaneous fracture of samples under the action of accumulated stresses.

Such fracture corresponds to the theory of the mine percussion nature [6]. In a general case, the condition for occurrence of a mine percussion is written in a form of inequality

$$N > T = \alpha\lambda\sigma_c, \qquad (2)$$

where N and T are the total normal and tangential stresses in the sample, Pa; λ is the stress range taken equal to depth h of the hole, m; α is dimensionless function λ depending on the form of working (for $\lambda \approx h$, α is taken equal to 0.5); σ_c is the ultimate strength for uniaxial compression, Pa.

Thus, appearance of disturbed zones in the samples will take place in the regions where the stress equal to

$$T = 0{,}5 \cdot 15 \cdot 150 \cdot 10^6 = 1{,}125 \cdot 10^9 \ \text{Pa}$$

is exceeded.

Having set up the mapping of isolines in the obtained samples in such a way that the lower limit of isolines was equal to the obtained value, it is possible to outline the fracture zones of the granite body (Fig. 17).

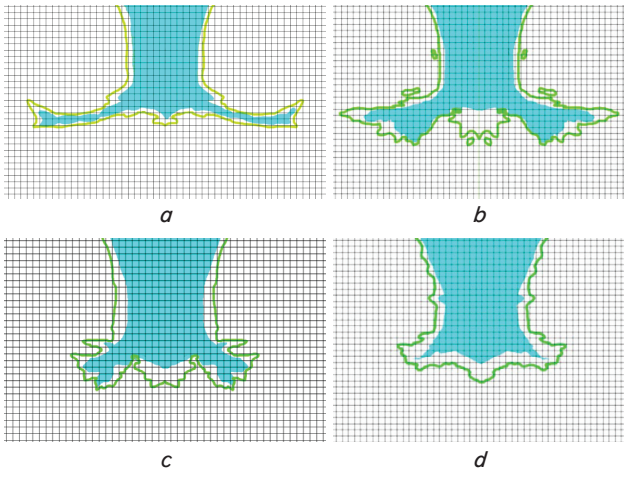

Fig. 17. Distribution of detonation products in the sample (the blue zone) and isolines of the normal stress with a lower threshold of $1.125 \cdot 10^9$ Pa (the green line) in the longitudinal section of a granite body with a size grid (grid pitch of 25 mm): *a* – r_r=0; *b* – r_r=10 mm; *c* – r_r=20 mm; *d* – r_r=40 mm

Analysis of the resulting fracture zones (Fig. 17, 18) makes it possible to draw the following conclusions:

– the change in the relative borehole bottom rounding radius $\bar{r}_r = r_r/D_0$ from 0 to 0.04 has no significant affect on the relative radius of the fracture zone at the level of the borehole bottom: if it is assumed that for $r_r \to 0$ it is equal to $\bar{R}_{cr} = 1$, then for r_r=0.04 this radius is equal to 0.9.

– an increase in the rounding radius from 20 mm ($\bar{r}_r = 0.08$) to 40 mm ($\bar{r}_r = 0{,}16$) results in a significant decrease in the relative radius of the fracture zone, namely:

$$\bar{R}_{cr} = 0.67 \ \text{at} \ \bar{r}_r = 0.08,$$

$$\bar{R}_{cr} = 0.61 \ \text{at} \ \bar{r}_r = 0.16;$$

– reduction of the borehole bottom rounding radius results in a decrease in the relative average width of the disc-shaped fracture zone: it is 1 for $r_r \to 0$ and 1.67; 2 and 1.33 for r_r=10, 20, 40 mm respectively. Consequently, presence of a stress concentrator makes it possible to form a narrower and longer initial crack.

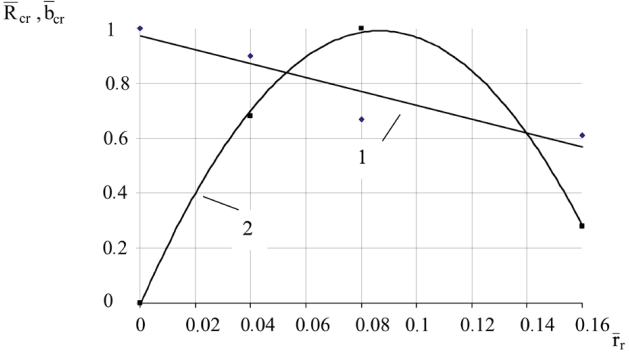

Fig. 18. Change in the crack size depending on the rounding radius: 1 – change in the relative length $\bar{R}_{cr}$; 2 – change in the relative width $\bar{b}_{cr}$

7. Conclusions

The theoretical studies of features of crack formation and enhancement of the dynamic effect in the lower part of the explosive charge made it possible to reveal dependence of the character of crack formation in the lower rock layers on the relative radius of rounding between the bottom and the walls of the borehole. As a result of these studies, the following was established:

1. With a relative rounding radius $\bar{r}_{cr} \le 0.04$, a practically horizontal crack is formed (the slope of its plane is 12–15° to the horizontal inward the body).

2. The length of this crack decreases linearly with an increase in $\bar{r}_{cr}$.

3. Change in the relative width of the initial crack depending on $\bar{r}_{cr}$, is described by a polynomial of the second degree.

References

1. Naumets, I. V. Optymizatsyia burovzryvnykh rabot pri dobyche skalnykh stroitelnykh materialov [Text] / I. V. Naumets, S. V. Dyniak, I. V. Makhonia, A. S. Storchak // Informatsyonnyi biulleten ukrainskoho soiuza inzhenerov-vzryvnikov. – 2010. – Issue 3. – P. 11–12.

2. Dombaiev, Zh. G. Matematicheskaia model dvizhenyia produktov vzryva v shpure dlia obespecheniia protsessa napravlennogo razrusheniia gornykh porod [Text] / Zh. G. Dombaiev, V. N. Kovalevskii // Vestnik Buriatskogo gosudarstvennogo universiteta. – 2011. – Issue 9. – P. 249–252.
3. Gornaia entsiklopediia. Vol. 1 [Text] / Ye. A. Kozlovskii (Ed.). – Moscow: Sovetskaia entsiklopediia, 1984. – 560 p.
4. Vorobyov, V. V. Usileniie kvazistaticheskogo deistviia produktov detonatsii v donnoi chasti shpura [Text] / V. V. Vorobyov, M. V. Pomazan // Visnyk KDPU imeni Mykhaila Ostrohradskoho. – 2008. – Issue 5. – P. 154–157.
5. Naumenko, V. P. Soprotivleniie razrusheniiu listovykh metallov i tonkostennykh konstruktsii. Soobshchenie 1. Kriticheskiy obzor [Text] / V. P. Naumenko, I. V. Limanskii // Problemy prochnosti. – 2014. – Issue 1. – P. 25–49.
6. Paramonov, G. P. Gazodinamicheskiie protsessy v shpure pri napravlennom razrushenii gornykh porod [Text] / G. P. Paramonov, V. N. Kovalevskyi, Zh. G. Dombaev, A. E. Rumiantsev // Vzryvnoie delo. – 2012. – Issue 108/65. – P. 93–99.
7. Leshchynskyi, A. B. Sredstva i sposoby rassredotocheniia skvazhinnykh zariadov [Text] / A. B. Leshchynskyi, Ye. B. Shevkun // Dalnyi Vostok-1. – 2009. – Issue OB4. – P. 23–34.
8. Vorobyov, V. V. Izmeneniie parametrov zony treshchinoobrazovaniia v tverdoi srede pri mnogotochechnom initsiirovanii [Text] / V. V. Vorobyov, V. T. Shchetinin // Suchasni resursoenerhozberihaiuchi tekhnolohii hirnychoho vyrobnytstva. – 2008. – Issue 1/2008 (1). – P. 86–90.
9. Pomazan, M. V. O vliianii kumuliativnogo effekta v udlinennom zariade na izmeneniie stepeni prorabotki podoshvy ustupa [Text] / M. V. Pomazan // Visnyk Kremenchutskoho derzhavnoho politekhnichnoho universytetu imeni Mykhaila Ostrohradskoho. – 2009. – Issue 1/2009 (54). – P. 97–102.
10. Faserova, D. Numerical Analyses of Buried Mine Explosions with Emphasis on Effect of Soil Properties on Loading [Text]: PhD Thesis/ D. Faserova. – Cranfield University, 2006. – 239 p.
11. Follett, S. Blast Analysis of Composite V-shaped Hulls: An Experimental and Numerical Approach [Text]: EngD Thesis/ S. Follett. – Cranfield University, 2011. – 289 p.
12. Laine, L. Derivation of mechanical properties for sand [Text] / L. Laine, A. Sandvik // 4th Asia-Pacific Conference on Shock and Impact Loads on Structures. – Singapore, 2001. – P. 361–368.
13. MatWeb [Electronic resource]. – Available at: http://www.matweb.com/
14. Tawadrous, A. Hard Rocks Under High Strain-Rate Loading [Text]: PhD Thesis / A. Tawadrous. – Queen's University. Kingston, Ontario, Canada, 2010. – 187 p.
15. Singh, P. K. Rock Fragmentation by Blasting: Fragblast 10 [Text] / P. K. Singh, A. Sinha // 10-th International Symposium on Rock Fragmentation by Blasting. – New Delhi, India, 2012. – P. 213–221.
16. Ramsey, J. M. Hybrid fracture and the transition from extension fracture to shear fracture [Text] / J. M. Ramsey, F. M. Chester // Nature. – 2004. – Vol. 428, Issue 6978. – P. 63–66. doi: 10.1038/nature02333
17. Pilipets, V. I. Sposoby razrusheniia gornykh porod [Text]: uch. pos. / V. I. Pilipets. – Donetsk, 2000. – 178 p.
18. Dehghan Banadaki, M. M. Stress-wave induced Fracture in Rock due to Explosive Action [Text]: PhD Thesis / M. M. Dehghan Banadaki. – Department of Civil Engineering, University of Toronto, 2010. – 128 p.